VILNIUS TECH
Vilnius Gediminas Technical University

Geodesy and Cartography
ISSN 2029-6991 / eISSN 2029-7009
2022 Volume 48 Issue 3: 150–159
https://doi.org/10.3846/gac.2022.14777

UDC 528.8

AN APPRAISAL OF THE ECMWF REANALYSIS5 (ERA5) MODEL IN ESTIMATING AND MONITORING ATMOSPHERIC WATER VAPOUR VARIABILITY OVER NIGERIA

Swafiyudeen BAWA*, Olalekan Adekunle ISIOYE, Mefe MOSES, Lukman ABDULMUMIN

Department of Geomatics, Faculty of Environmental Design, Ahmadu Bello University, Zaria, Nigeria

Received 17 April 2021; accepted 02 September 2022

Abstract. This study research the performance of the ERA5 reanalysis model in estimating and monitoring the variability of atmospheric water vapour content over Nigeria. The ERA5 is a fifth-generation reanalysis model recently released by the European Centre for Medium-Range Weather Forecasts (ECMWF). The ERA5 model comes with excitingly high spatial and temporal resolution when compared to earlier models like the ERA-Interim and ERA-40. However, like the previous models, the ERA5 comes with numerous modelling uncertainties arising from data fusion methods and observation schemes, which often affects its performance at the different regions of the Earth. In this study, ERA5 precipitable water vapour (PWV) was validated with GNSS PWV from permanent GNSS stations in Nigeria NIGNET for the period of 2012–2013. The performance of ERA5 was investigated at sub-daily, diurnal, and seasonal scales in relation to Köppen-Geiger climate classification using standard statistical metrics (namely, coefficient of correlation (r), Root mean square error (RMSE), Reliability index (RI), Mean absolute errors (MAE) and mean bias). The r, RI, RMSE, MAE and mean bias values at sub-daily, diurnal and seasonal scales were computed as, (0.8670, 0.882, 0.979), (3.697 mm, 3.400 mm, 7.014 mm), (1.015, 1.019, 1.008), (2.769 mm, 2.706 mm, 1.939 mm) and (0.826 mm, 2.033 mm, 1.739 mm), respectively. The results indicate the strongest performance of ERA5 at seasonal scale with more than 95% agreement. The pattern of variability of ERA5 within the different climate zones of Nigeria showed good consistency with GNSS PWV and Köppen-Geiger climate classification. The study recommended the use of ERA5 in the retrieval of historic PWV records and near real-time GNSS applications.

Keywords: ERA5, Köppen-Geiger, NIGNET, PWV.

Introduction

Water vapour is a greenhouse gas and a very important atmospheric variable that drives, and affects global hydrological and climate processes (Isioye et al., 2015). Precipitable water vapour (PWV) or total column of water vapour (TCWV) are the terms often used by scientists as measures of this greenhouse gas. The PWV as adopted in this study is the atmospheric water vapour contained in a vertical column of the unit area from the Earth's surface to the uppermost part of the atmosphere. The PWV exhibits high spatio-temporal variability and due to its complex characteristics in both space and time, its measurement and modeling often tend to be difficult (Yang et al., 2019). The knowledge of the amount and variability of water vapour in the atmosphere is very important to climate studies and monitoring.

Water vapour is often measured by ground and space-based systems. The ground-based systems (e.g., GNSS, sun photometry, radiosonde and microwave radiometry) provide in-situ measurement and are mostly limited by the sparseness of observation systems across the globe. Radiosondes, ground and satellite-based radiometry have some limitations but not limited to their expensive nature, calibration error, poor temporal resolution and data quality, unlike their GNSS counterpart (Choy et al., 2015). The spaced-based systems (such as MODIS, COSMIC/FORMOSAT-3 and atmospheric infrared sounder (AIRS), etc.), which are used to make observations from satellites in space, provide wider coverage as compared to ground systems but are limited by their temporal resolutions.

The GNSS over the past and the present time has shown great potential in the retrieval of water vapour

*Corresponding author. E-mail: *bswafiyudeen@gmail.com*

in the atmosphere (Davis et al., 1985; Bevis et al., 1992, 1994; Gurbuz et al., 2015; Isioye et al., 2016) due to its high accuracy, all-weather capability, high spatial and temporal resolution. Although the spatial resolution of GNSS is a concern in many regions of the world like Africa. Ground-based GNSS meteorology can be advantageous in numerical weather forecasting and assimilation. Regionally and globally, it can be adopted for climate monitoring and atmospheric research, and in the validation of satellite and numeric products (Ansari et al., 2018).

Several numerical weather models (NWMs) of different generations from the European Centre for Medium-Range Weather Forecasts (ECMWF) and National Centre for Environmental Prediction (NCEP)/National Centre for Atmospheric Research (NCAR) have evolved over the years. The NWMs are based on prediction models and the integration of data from different sources (Ojigi & Opaluwa, 2019; Zhang et al., 2019). This, as a result, makes such models erroneous due to variation of the models, fusion method and observation schemes (Ssenyunzi et al., 2020; Yang et al., 2019). The accuracy of the models vary from one region to another, thus, there is a need to validate their performance over the different region (Ansari et al., 2018; Isioye et al., 2017; Ojigi & Opaluwa, 2019; Xiaoming et al., 2010; Yang et al., 2019). Although, GNSS-based PWV is rarely used in NWM reanalysis data models, but most often used in validations. It is worth mentioning that the non-availability of meteorological sensors at some GNSS stations affects the accuracy of PWV estimations. In such cases, numerical weather prediction (NWP) models are used to retrieve empirical tropospheric mapping function such as VMF1 (Boehm et al., 2006) and VMF3 (Landskron & Böhm, 2018). Several studies (see, for example Jade & Vijayan, 2008) have demonstrated the feasibility of using GNSS in PWV estimation to an accuracy of up to 2 mm and validated the NCEP based PWV with the GNSS based ones.

In Nigeria, the study of Abimbola et al., (2017) found a weak correlation between GNSS PWV of some NIGNET stations operated and maintained by the Office of the Surveyor General of the Federation (OSGOF), and the NCEP/DOE Reanalysis II – the time series of each of the PWV sources exhibited an identical pattern. Lack of meteorological sensors attached to NIGNET and the poor resolution of NCEP/DOE was attributed to the weak correlation. In Ghana, Acheampong et al. (2015) found a correlation of more than 60% when PWV from GNSS was compared with that from the NCEP/DOE Reanalysis II. The study of Isioye et al. (2017) capitalized on the NIGNET to study spatio-temporal variability of PWV. Out of the 15 NIGNET stations across Nigeria, Isioye et al. (2017) used five and recorded a strong interrelation among GNSS, AIRS and ERA-Interim based models. In another study by Ojigi and Opaluwa (2019) NCEP/DOE and ERAI were compared against each other and more than 90% correlation was recorded.

The release of the fifth generation ECMWF ReAnalysis5 (ERA5) hourly data and spatial resolution of 31 km provides the opportunity for monitoring PWV at a temporal scale like never before from any reanalysis model. Studies from different parts of the world have shown good results for the ERA5. In the tropical region of East Africa, Ssenyunzi et al. (2020) conducted an assessment of ERA5 PWV retrieval and validated it with ground-based GNSS – about 90% correlation was observed. Yang et al. (2019) also conducted an appraisal of ERA5 PWV with ground-based GNSS in China; about 95% correlation was recorded.

This study research the potential of the ERA5 in estimating PWV over Nigeria for real time GNSS applications. Thus, GNSS PWV was utilized in the performance appraisal of ERA5. The study provides in-depth knowledge of the temporal variability (i.e., sub-daily diurnal, and seasonal scales) of PWV due to the unique capability of ERA5 over previously validated models in Nigeria. In this paper, we first describe the data used for validating the ERA5 and methodology (Section 1). The results and discussions of the results are in Section 2. Finally, the conclusions and recommendations are given in the last Section.

1. Data and methodology

1.1. Study area

Nigeria (Figure 1), situated in the Western part of Africa is located between latitude 4 °N and 14 °N and longitude 2 °E and 14 °E. This country is bordered by the Atlantic Ocean (to the South), Niger Republic and Chad (to the North), Benin Republic (to the West) and Cameroon (to the East). It is characterized by high (low precipitation) and low (high precipitation) elevations in the Northern and Southern part respectively. There are basically two seasons: dry season and the rainy season. Base on Köppen-Geiger climatic classification (Kottek et al., 2006; Beck et al., 2018) Nigeria has 6 climatic classifications (Figure 2): Tropical Rainforest (Af) around the extreme coast of the Niger Delta (Bayelsa, Rivers and AkwaIbom);

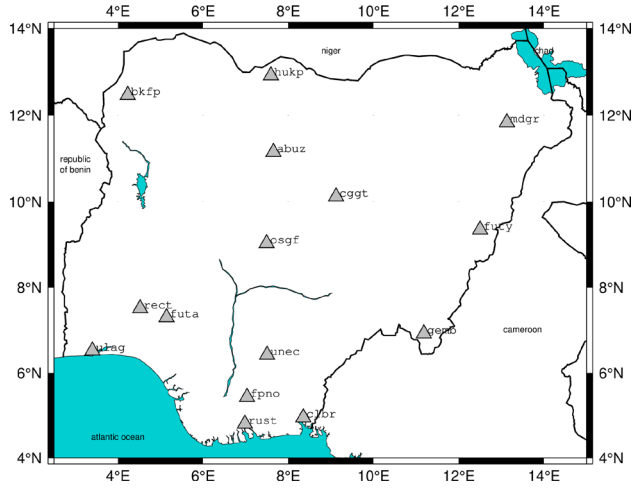

Figure 1. Map of Nigeria depicting the GNSS stations used for the study (Bawa et al., 2021)

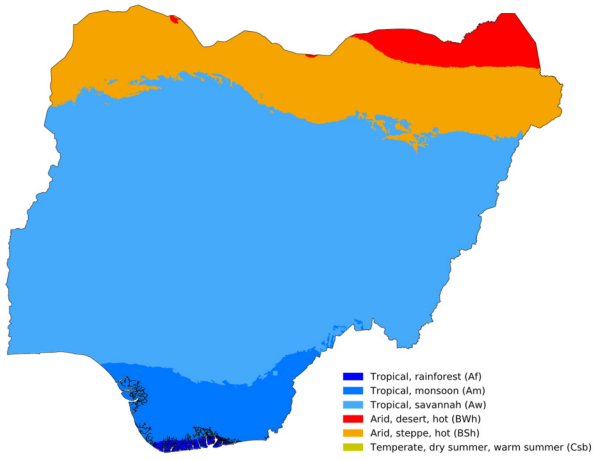

Figure 2. Köppen-Geiger climate classification for Nigeria; 1980–2016 (Beck et al., 2018)

Tropical Monsoon (Am) around Edo, Enugu, Imo, Abia and Cross River; Tropical Savannah (Aw) around North-Central and South-West geopolitical zones; Arid Desert hot (BWh) around some part of North-East geopolitical zone; Arid Steppe hot (BSh) around the North-West geopolitical zone.

1.2. Dataset

Ground-based GNSS tropospheric data spanning 2012–2013 of NIGNET were processed by and downloaded from Nevada Geodetic Laboratory (NGL) (Blewitt et al., 2018). The NGL provides more than 43,000,000 station-days of tropospheric products (which include: water vapour, weighted mean temperature, total zenith delay, north and east gradient) at every 5 minutes since 1994 to present from over 18,000 GNSS stations across the globe using GIPSY/OASIS-II software developed by the Jet Propulsion Laboratory (JPL). A summary of the parameters used in estimating PWV is presented in Table 1. Other processing parameters can be found via http://geodesy.unr.edu/gps/ngl.acn.txt. A summary of the characteristics of the data set used is presented in Table 2.

Hourly ERA5 data spanning 2012–2013 were downloaded from ECMWF website in NetCDF format. Information about ERA5 can be found via https://www.ecmwf.int/en/forecasts/datasets/reanalysis-datasets/era5.

Table 1. Parameters used in computing PWV by NGL

Parameter(s)	Description
Method	Precise point positioning (PPP)
Elevation angle cutoff	7 °
Sampling rate	5 minutes
Wet and dry mapping function	Vienna mapping function VMF1
Integrated water vapor	Wet zenith delay using Bevis et al. (1994) refractivity coefficients

Table 2. Characteristics of data set used for the study

Data file and type	Spatial and temporal resolution		Data source
ERA5	0.25 °×0.25 °	1 hour	ECMWF*
SINEX tropospheric		5 minutes	NGL**

Notes: ** http://geodesy.unr.edu/gps_timeseries/trop/

* https://www.ecmwf.int/en/forecasts/datasets/reanalysis-datasets/era5

1.3. Determination of PWV from GNSS and NWM

To the Geodesist, the atmospheric errors caused by the troposphere are a concern but for meteorological studies, the tropospheric error is useful for climate studies and other related applications. The delay caused by the troposphere called Zenith Total Delay (ZTD) can be divided into two parts: the non-hydrostatic (wet) part (ZWD) which is water vapour and temperature dependent and the hydrostatic (dry) part (ZHD) which is surface pressure dependent (Gurbuz et al., 2015; Mengistu-Tsidu et al., 2015). The ZHD amounts to about 90% of the ZTD. The path length taken by satellite signal to the receiver which is also termed ZTD can be expressed as Equation (1).

$$\mathrm{ZTD} = 10^{-6} \int N(s)\,ds, \tag{1}$$

where $N = 10^6(n-1)$ is the atmospheric refractivity, n is refractive index. A more accurate expression is provided in Bevis et al. (1994) as $N = k_1 \frac{P_d}{T} + k_2 \frac{P_v}{T} + k_3 \frac{P_v}{T^2}$.

Equation 1 can also be expressed as Equation (2):

$$\mathrm{ZWD} + \mathrm{ZHD} = \mathrm{ZTD}. \tag{2}$$

The ZHD in Equation (2) can be computed using surface meteorological data given in Equation (3) as (Saastamoinen, 1972; Davis et al., 1985):

$$\mathrm{ZHD}(\rho_s, \lambda, h) = \frac{p(2.2779 \pm 0.0024)}{(1 - 0.00266\cos(2\lambda) - 0.00028h)}, \tag{3}$$

where p is the total pressure at the Earth's surface in millibars, λ is latitude of antenna and h is station's altitude above the ellipsoid in kilometres. This is a function of latitude. However, ZWD is mostly inaccurately calculated due to the dispersed and unpredictable water vapour content in the atmosphere. The errors budget can reach up to several centimetres at the zenith. It can be calculated by subtracting ZHD from ZTD, as given in Equation (4).

$$\mathrm{ZWD} = \mathrm{ZTD} - \mathrm{ZHD}. \tag{4}$$

Once ZWD is estimated, PWV can be computed. PWV is roughly proportional to ZWD, given by Equation (5):

$$\mathrm{PWV} = \Pi \times \mathrm{ZWD}. \tag{5}$$

Π is a proportionality constant that is dimensionless. This is given by Equation (6):

$$\Pi^{-1} = 10^{-6}\left(k_3 T_m^{-1} + k_2^{'}\right) R_v \rho_v, \tag{6}$$

where $k_2^{'}$ and k_3 are refractivity constants with values 22.1±2.2 K/mbar, and 373 900±12 000 K^2/mbar respectively. R_v is the specific gas constant for water vapour with the value 461.524 $Jkg^{-1}K^{-1}$ (Bevis et al., 1992). The parameter T_m in Equation (6) is the weighted mean temperature depending on surface temperature T_s given by Bevis et al. (1994).

$$T_m = 0.72T_s + 70.2. \tag{7}$$

The PWV can be estimated from vertical profiles of a reanalysis model using the relation (Jiang et al., 2016):

$$\mathrm{PWV} = \int_{surface}^{atmosphere} \frac{q}{\rho_w g} dp. \tag{8}$$

In Equation (8) ρ_w is the density of liquid water, p is air pressure, q is the specific humidity and g is acceleration due to gravity given by 9.80665 m/s^2.

1.4. Methodology

Hourly ERA5 PWV retrieved from ECMWF website was sorted accordingly for sub-diurnal estimation. Thereafter, GNSS PWV of 5minutes temporal scale were averaged into their ERA5 sub-diurnal (1hour) equivalence. Also, hourly ERA5 and NGL PWV were averaged into diurnal temporal scale. And finally, ERA5 and NGL diurnal data were grouped and averaged into seasonal (DJF, MAM, JJA, SON) temporal scale. Nearest Neighbour interpolation scheme was employed in obtaining corresponding ERA5 PWV of the NIGNET stations.

Five statistical metrics were utilized to assess the performance of the two datasets. These include: mean bias (MB), mean absolute error (MAE) (Shcherbakov et al., 2013), root mean square error (RMSE), reliability index (RI) (Leggett & Williams, 1981), correlation coefficient (r). Observed value (x_i) is assigned to the GNSS data from NGL whereas the model estimates (y_i) is assigned to the ERA5. N is the number of observations.

$$\mathrm{MB} = \frac{1}{N}\sum_{i=1}^{N}(x_i - y_i); \tag{9}$$

$$\mathrm{MAE} = \frac{\sum_{i=1}^{N}|x_i - y_i|}{N}; \tag{10}$$

$$\mathrm{RMSE} = \sqrt{\frac{\sum_{1}^{N}(x_i - y_i)^2}{N}}; \tag{11}$$

$$\mathrm{RI} = \exp\sqrt{\frac{\sum_{i=1}^{N}\left(\ln\left(\frac{x_i}{y_i}\right)\right)^2}{N}}; \tag{12}$$

$$r = \frac{\sum_{i=1}^{N}(x_i - \hat{x})(y_i - \hat{y})}{\left[\sum_{i=1}^{N}(x_i - \hat{x})^2 \cdot \sum_{i=1}^{N}(y_i - y)^2\right]^{1/2}}. \tag{13}$$

2. Results and discussions

In this study, PWV estimate from GNSS and ERA5 reanalysis model were investigated at sub-daily, diurnal and seasonal scales to ascertain the suitability of the ERA5 in predicting and monitoring PWV variations over Nigeria. The evaluation was carried out using data from the period of 2012–2013.

2.1. Sub-daily variation

Variation in PWV is dependent on latitude, topography, seasons and continental air masses resulting from massive land and sea breeze convergence (Isioye et al., 2019). Figures 3 and 4 present heat maps of the variations in PWV in 2012 and 2013 over the corresponding NIGNET stations derived from ERA5 at monthly/seasonal (see vertical axis) period and at hourly temporal scale (see horizontal axis).

Based on the Köppen-Geiger climatic classification as presented in section 2.1, Figures 3 and 4 show that stations RUST, FPNO and CLBR located around the Tropical Monsoon (Am) region recorded the most the atmospheric water content. This is followed by stations ULAG and UNEC located around the Tropical Savannah (see Figures 1 and 2) which both exhibit similar high atmospheric PWV to stations RUST, FPNO and CLBR which are located around the Tropical Monsoon (Am) region (see also Figures 1 and 2). In Figures 3 and 4, the variation of PWV at a particular time of the day is dependent on the season, month and year. For example, station RUST in Figure 3, for January, recorded a decrease in atmospheric water vapour from 0–12 hours (UTC) – the PWV increases from 12–21 hours (UTC); then another decrease from 21–23 hours (UTC). This is relatively different from what is attainable for the same station in Figure 4 for year 2013. From the Tropical Monsoon to the Tropical Savannah, a decrease in atmospheric water vapour content is observed over the stations in these regions (Figures 3 and 4). Stations MDGR, BKFP and HUKP (Figures 1–4) in the arid dessert steppe, experience the lowest atmospheric water vapour content throughout the year.

Figures 5 and 6 present corresponding PWV over the NIGNET stations from NGL. Stations with less than 5 months data were excluded from the plots – this is a major setback of the NIGNET data (data gap) from NGL. Ideally, it is expected that Figures 3 and 5, and 4 and 6 portray similar pattern. For better understanding of their relationship, the monthly/seasonal variations of the 2 datasets are researched. Across the stations as depicted in Figures 3, 4, 5 and 6 between the two PWV sources, irrespective of the time of day, the lowest peak of monthly PWV was recorded in January, February and March the months. Although, stations in the Southern part of the country – mostly tropical Rainforest and Monsoon, exhibited relatively high PWV during these months vis-à-vis their Northern counterparts. It is also observed that PWV reaches its peak in August, September and October for the stations located in the

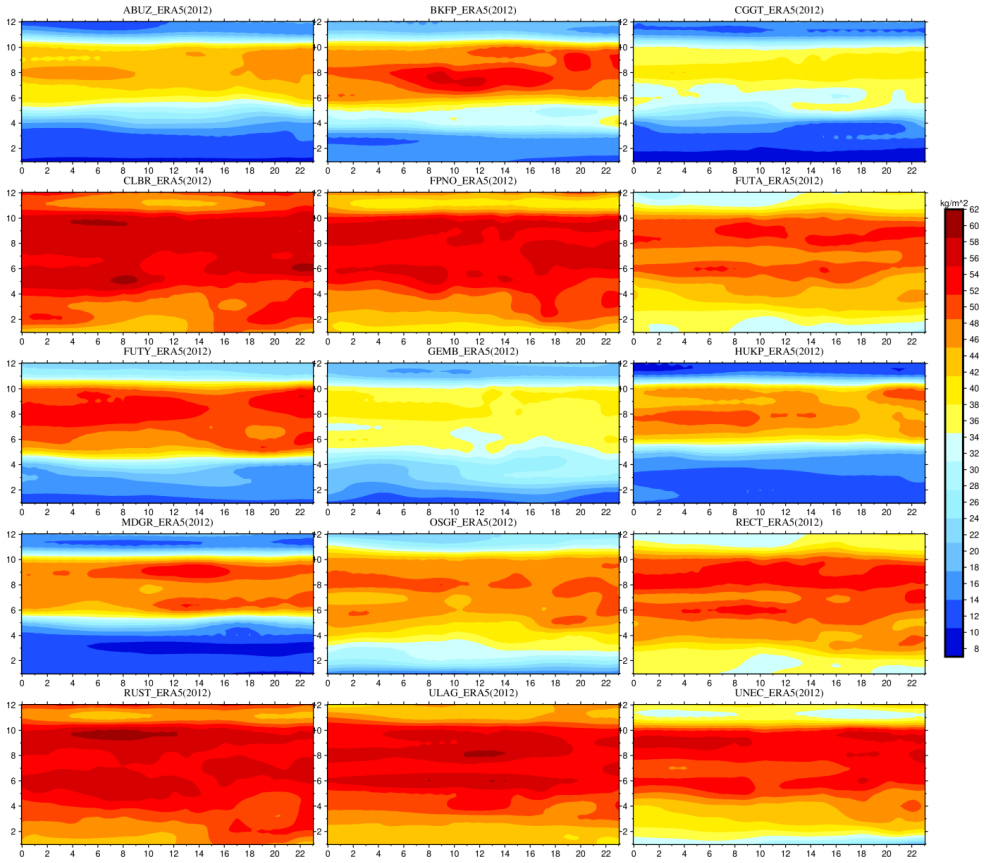

Figure 3. Sub-daily variation of ERA5 PWV (kg/m^2) over 15 CORS for year 2012, plots are months against time (UTC hours)

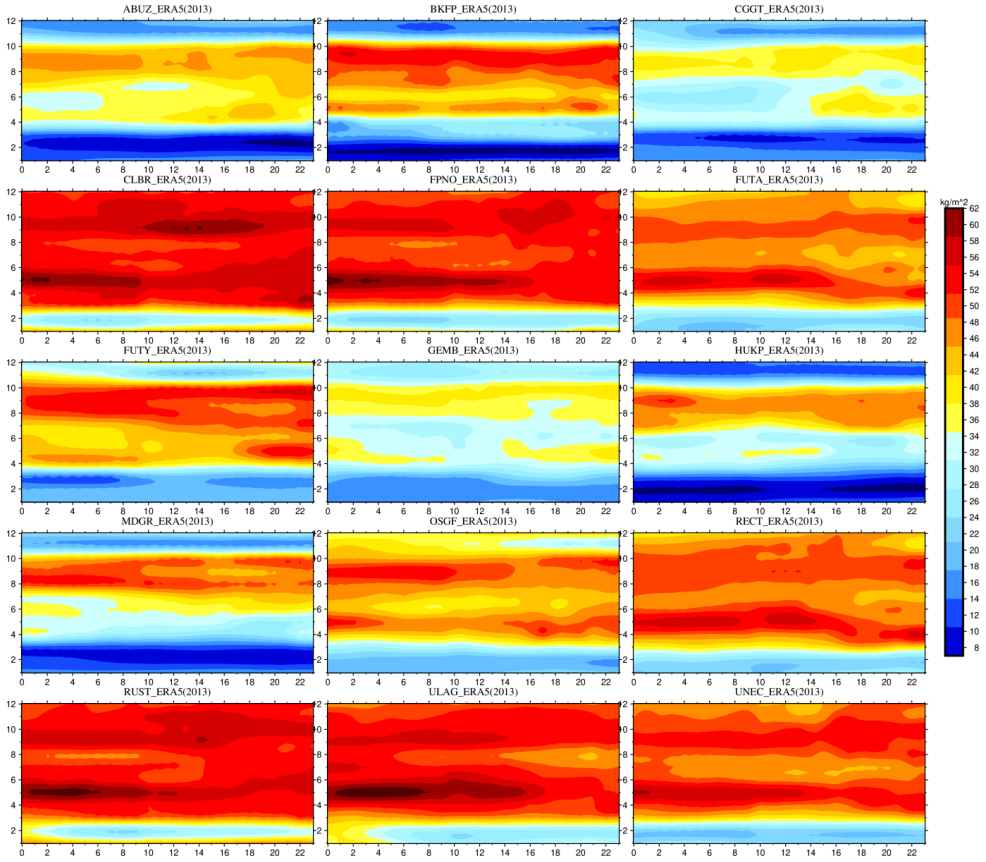

Figure 4. Sub-daily variation of ERA5 PWV (kg/m^2) over 15 CORS for year 2013, plots are months against time (UTC hours)

central part of the country (ABUZ, CGGT, OSGF, FUTY and GEMB). Stations MDGR, HUKP and BKFP also exhibit similar characteristics (Figures 3–6). This is as against stations RECT, FUTA and UNEC which depict varying peaks from mid-May to October. Stations CLBR, RUST and ULAG located relatively very close to the coast of Nigeria exhibited very high PWV between 42–62 kg/m^2 (or mm, because 1 kg of water corresponds to 1 dm^3 of water) from February to December – peaks at these stations are mostly observed around the month of May at 0–9 hour (UTC) – this corroborates the study of Ojigi and Opaluwa (2019).

2.2. Diurnal and seasonal variation

In this section, the daily and seasonal PWV variability over Nigeria is investigated. Figure 7 presents the diurnal variation of PWV from GNSS and ERA5 over the selected stations aggregated from hourly mean of each day. A seasonal trend is observed over the selected sites. It can be observed that the ERA5 and GNSS PWV mimic similar trend but how well they agree is discussed in section 2.3.

In the present study, it was observed that characterizing the seasonal variation of PWV from the aggregated

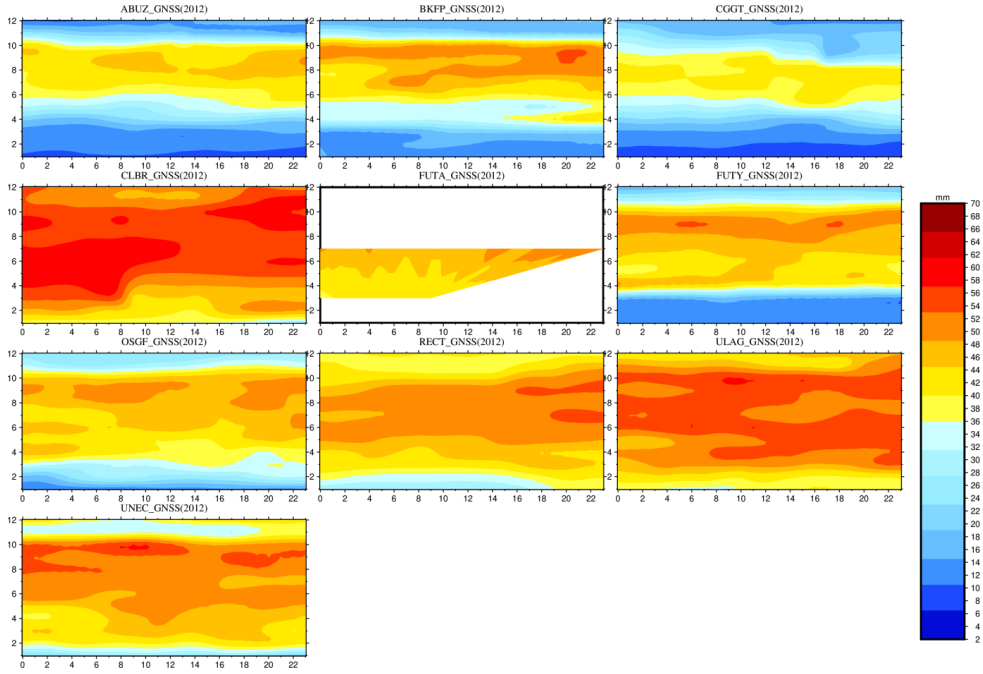

Figure 5. Sub-daily variation of GNSS PWV (mm) over 15 CORS for year 2012, plots are months against time (UTC hours)

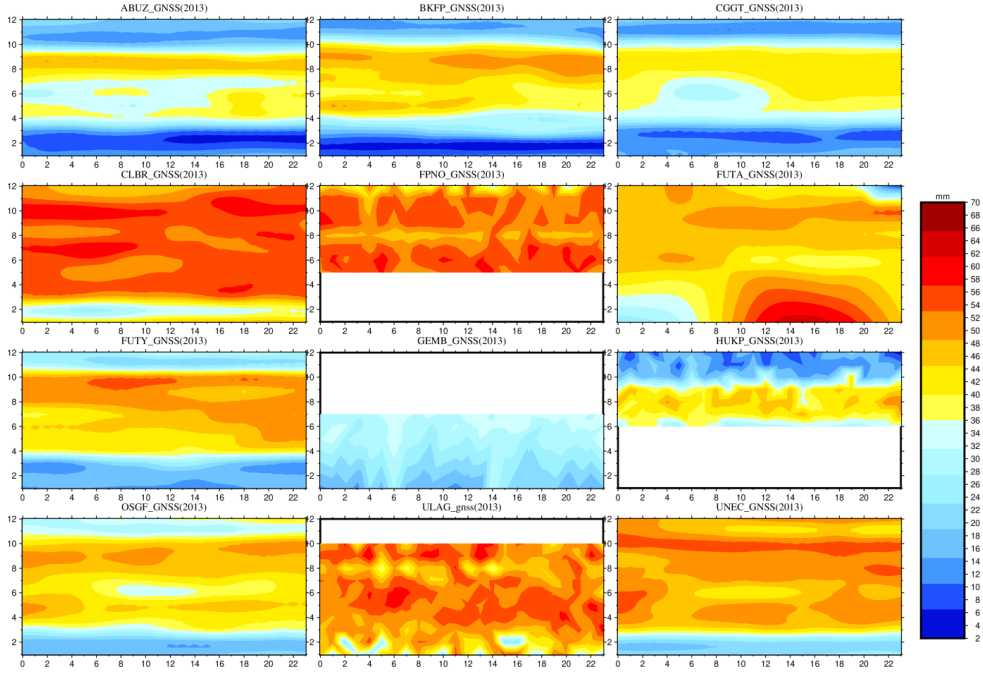

Figure 6. Sub-daily variation of GNSS PWV (mm) over 15 CORS for year 2013, plots are months against time (UTC)

monthly mean (Figure 8) produced a more reasonable pattern than can be interpreted from the sub-daily plots (Figures 3–6). Figure 8 depicts the PWV values for the four seasons experienced in Nigeria: March, April and May (MAM); June, July and August (JJA); September, October and November (SON); and December, January and February (DJF).

As presented in Figure 8, the seasons MAM and DJF are characterized by dry seasons, while JJA and SON are characterized by wet seasons. The MAM and DJF exhibit low PWV, but the MAM season has high PWV when compared to the DJF season. Toward the Northern part of the country, the MAM season exhibit low PWV, while the Southern part of the country exhibits a relatively high PWV compared to their Northern counterpart. Figure 8a and 8b also show very high PWV (both in the Northern and Southern part of the country in the JJA season. The JJA for the 2 data sets exhibited the highest PWV amongst the 4 seasons. The wet season is at its peak in these months. The PWV is between 34 to 62 kg/m^2 (mm) from the Southern to the Northern part of the country. The SON season is the season that marks the beginning of decrease in PWV across the country. On the contrary, this season marks the end of the rainy season in the Southern region, it's a season characterized by little rainfall and enormous amount of thunderstorm. It is indicative that PWV is season dependent. This corroborates the observations of Ansari et al. (2018), Isioye et al. (2017), Ssenyunzi et al. (2020).

2.3. Statistical validation

Figures 9 and 10 respectively present the sub-daily and diurnal performance metrics of ERA5 against NGL PWV for each station under research. This would give a better insight on how well ERA5 performs in the sub-daily and

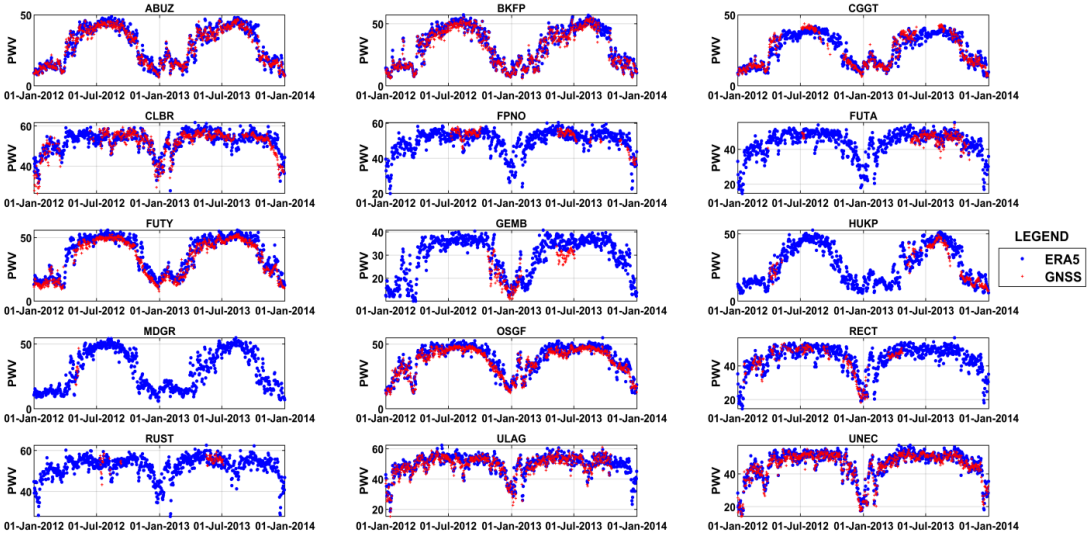

Figure 7. Diurnal variation of PWV derived from GNSS and ERA5 during the period 2012–2013. Units are in mm or kg/m^2

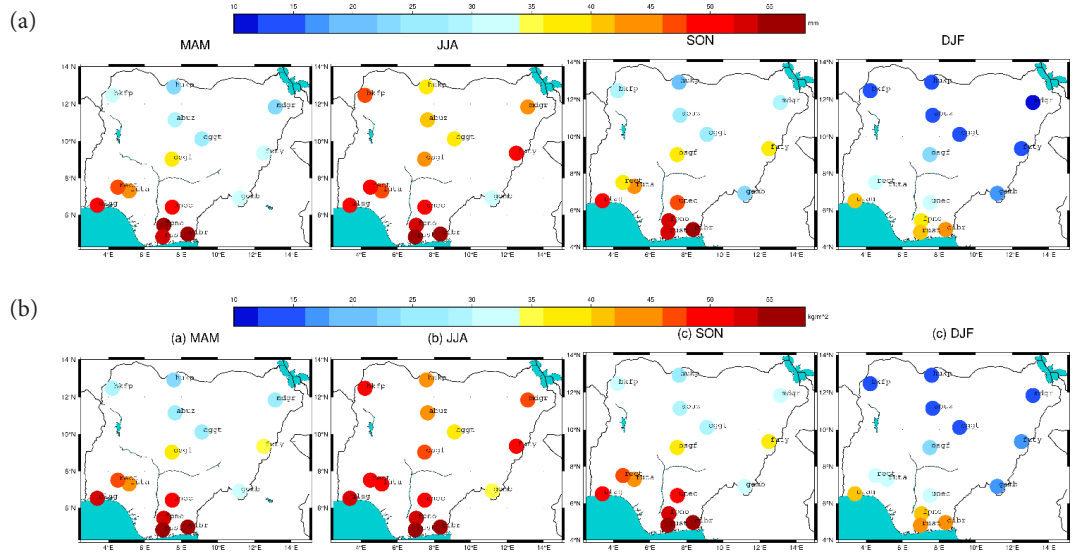

Figure 8. Seasonal means: a – GNSS PWV (mm); b – ERA5 PWV (kg/m^2) for MAM, JJA, SON, and DJF from 2011–2013

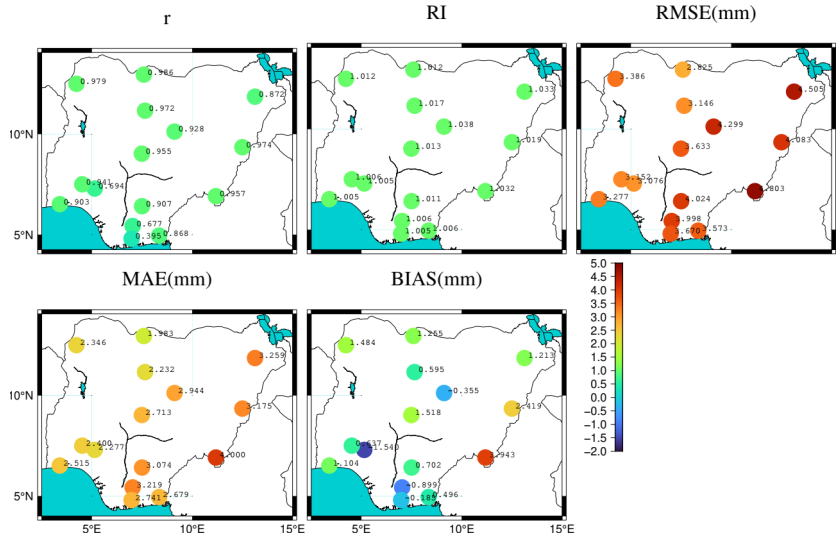

Figure 9. Statistical plot of sub-daily agreement of PWV from ERA5 and GNSS from 2012–2013

diurnal scale. In the present study, r explains how much variability can be found between ERA5 and GNSS. The correlation coefficient (r) of GNSS PWV and ERA5 at sub-daily scale are illustrated at the top left of Figures 9 and 10. In Figure 9, the r mimics no clear pattern but stations FPNO (0.677) and FUTA (0.694) had r values of less than 70% with station RUST having the worst r value of 0.395 (less than 40%).

An improvement is noticed in Figure 10, which is the mean aggregate of hourly PWV from GNSS and ERA5. Exceptions to this improvement is noticed at stations FUTY, HUKP, MDGR and RECT. The r values for these stations decreased from 0.974 to 0.959 for station FUTY, 0.986 to 0.935 for station HUKP, 0.872 to 0.779 for station MDGR and 0.941 to 0.924 for station RECT for the sub-daily and diurnal scale respectively.

Average r values for the sub-daily trend were computed as 0.867, while average r values for the diurnal trend were computed 0.882. This implies that at diurnal scale, ERA5 has the tendency of better predicting the PWV over Nigeria.

RI measures how much two models differ from each other. Values close to 1 indicate close match. The mean RI values at individual stations in Figure 9 between ERA5 and GNSS PWV (at sub-daily scale) are in the range 1.005 to 1.038 with an overall value of 1.015. Similarly, the mean RI values at individual stations in Figure 10 between ERA5 and GNSS PWV (at diurnal scale) are in the range 1.003 to 1.062 with an overall value of 1.019. We can observe that the overall values for both sub-daily and diurnal scale are relatively equal-this shows how promising is ERA5 in retrieving PWV at hourly temporal scale.

RMSE is a measure of average square. It defines how close two models are. It ranges from 0 to infinity. Zero values are optimum. The RMSE values are in the range 2.825 to 4.804 mm (at sub-daily scale) with average value of 3.697 mm (Figure 9). At the diurnal scale (Figure 10), RMSE values are in the range 1.689 to 5.373 mm, with average value of 3.400 mm.

MAE on the other hand measures the absolute deviation between two compared entities. Similar to the RMSE,

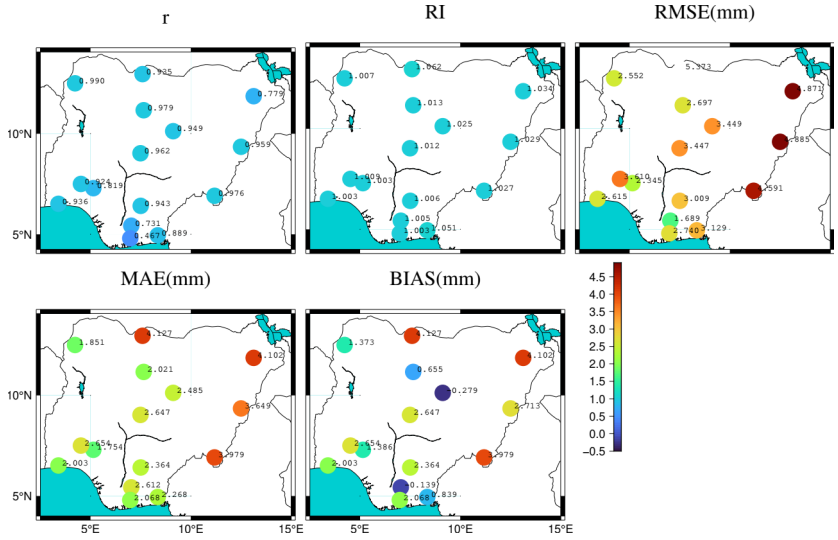

Figure 10. Statistical plot of diurnal agreement of PWV from ERA5 and GNSS from 2012–2013

values near zero indicate coincidence between observed and forecasted model. The MAE values are in the range 1.983 to 4.000 mm (at sub-daily scale) with average value of 2.770 mm. At the diurnal scale, MAE values are in the range 1.754 to 4.127 mm, with average value of 2.706 mm.

On a general note, bias defines the level at which PWV from ERA5 and GNSS are over or underestimated. It ranges from –1 to 1 and optimum values are at 0. At sub-daily scale, bias values are in the range –1.540 to 3.943 mm with average value of 0.826 mm. At the diurnal scale, the observed range is –0.139 to 4.127 with average value of 2.033 mm.

Table 3. Seasonal statistics of ERA5 and NGL PWV

Season	r	MAE	RMSE	RI	Bias
DJF	0.996	1.421	3.048	1.006	1.319
MAM	0.993	1.308	2.328	1.002	0.614
JJA	0.966	1.823	5.724	1.004	1.823
SON	0.963	3.205	16.955	1.020	3.200
Mean	0.980	1.939	7.014	1.008	1.739

Table 3 shows the seasonal statistics of PWV from the two data sources. With r values of up to 99%, it is obvious that ERA5 predicts very well the PWV of the season DJF. This is followed by the MAM season. The JJA and SON seasons had r values of 0.966 and 0.963 respectively. Similarly, the seasons of DJF and MAM recorded the lowest MAE, RMSE, RI and bias. Whilst the seasons of JJA and SON recorded the highest MAE, RMSE, RI and bias. Possible reason for this slight difference is that ERA5 performs poorly in humid regions (Ssenyunzi et al., 2020); therefore, the seasons of JJA and SON are quite humid compared to the seasons of DJF and MAM.

The performance indices, for the sub-daily and diurnal scale are summarized as (see also Figure 11):

1. Overall r, RI, RMSE, MAE and bias values for the sub-daily scale were computed as 0.867, 1.015, 3.697 mm, 2.769 mm and 0.826 mm respectively;
2. The overall r, RI, RMSE, MAE and bias values for the diurnal scale were computed as 0.882, 1.019, 3.400 mm, 2.706 mm and 2.033 mm respectively;
3. Finally, r, RI, RMSE, MAE and bias values for the seasonal scale were computed as 0.979, 1.008, 7.014 mm, 1.939 mm and 1.739 mm respectively.

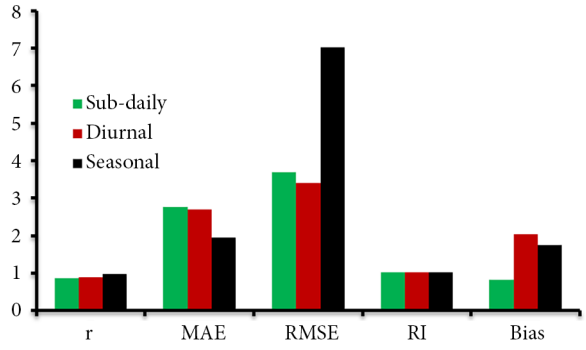

Figure 11. Aggregated performance indices

Conclusions

We investigated the performance of PWV over Nigeria from recent hourly ERA5 reanalysis data and ground-based GNSS PWV estimates from NGL, with a view to ascertain the performance of the new fifth generation ERA5 in estimating PWV over Nigeria, which has improved spatial and temporal resolution. The PWV from the reanalysis data were investigated against the GNSS data sets based on sub-daily, diurnal and seasonal scale.

Stations located around the Af exhibit high PWV. The BWh and BSh experience the lowest atmospheric water vapour content. These are all dependent on the time of the day, season, month and year.

We have also classified PWV estimates based on the data into MAM, JJA, SON, and DJF, with a view to study the seasonal relationship of PWV in Nigeria. The JJA season is characterized as having highest PWV amongst the four seasons. Though, the seasonal variability is a function of geographic latitude and Köppen-Geiger climate classification of Nigeria. However, possible reason for large differences in performance indices for some stations is due to the limitations of the ECMWF in humid regions and large height difference in reducing PWV (Ssenyunzi et al., 2020). From Figure 11, it appears that at seasonal scale, ERA5 better predicts the atmospheric PWV. This is followed by the diurnal and then the sub-daily estimate.

Mostly, GNSS stations are collocated with meteorological sensors so as to enable real time PWV estimation. On the contrary, the NIGNET stations lack meteorological sensors; this makes it difficult for real time meteorological applications. Therefore, this study is an indication that ERA5 can support real time applications of PWV retrieval without contaminating sub-daily cycles. For historical PWV retrieval at GNSS stations without collocated meteorological sensors, ERA5 can be an alternative.

Acknowledgements

The authors appreciate Nevada Geodetic Laboratory for the GNSS tropospheric data. Special thanks also to the European Centre for Medium-Range Weather Forecasts (ECMWF) for providing ERA5 data. Maps were generated with Generic Mapping Tool (GMT) (Wessel et al., 2019). Big thanks to Fatima Abdullahi Kudu for providing the work station used for the study.

References

Abimbola, O. J., Falaiye, O. A., & Omojola, J. (2017). Estimation of precipitable water vapour in Nigeria using NIGNET GNSS/GPS, NCEP-DOE reanalysis II and surface meteorological data. *Journal of Physical Science*, *28*(2), 19–29. https://doi.org/10.21315/jps2017.28.2.2

Acheampong, A. A., Fosu, C., Amekudzi, L. K., & Kaas, E. (2015). Comparison of precipitable water over Ghana using GPS signals and reanalysis products. *Journal of Geodetic Science*, *5*(1). https://doi.org/10.1515/jogs-2015-0016

Ansari, K., Corumluoglu, O., Panda, S. K., & Verma, P. (2018). Spatiotemporal variability of water vapor over Turkey from GNSS observations during 2009–2017 and predictability of ERA-Interim and ARMA model. *The Journal of Global Positioning Systems*, *16*(1), 8. https://doi.org/10.1186/s41445-018-0017-4

Bawa, S., Ojigi, L. M., Dodo, J. D., & Lawal, K. M. (2021). Strain rate field on the Nigeria lithosphere derived from GNSS velocity. *Applied Geomatics*, *13*, 179–193. https://doi.org/10.1007/s12518-020-00336-1

Beck, H. E., Zimmermann, N. E., McVicar, T. R., Vergopolan, N., Berg, A., & Wood, E. F. (2018). Present and future Köppen-Geiger climate classification maps at 1-km resolution. *Scientific Data*, *5*(1), 1–12. https://doi.org/10.1038/sdata.2018.214

Bevis, M., Businger, S., Chiswell, S., Herring, T. A., Anthes, R. A., Rocken, C., & Ware, R. H. (1994). GPS meteorology: Mapping zenith wet delays onto precipitable water. *Journal of Applied Meteorology*, *33*(3), 379–386. https://doi.org/10.1175/1520-0450(1994)033<0379:GMMZWD>2.0.CO;2

Bevis, M., Businger, S., Herring, T. A., Rocken, C., Anthes, R. A., & Ware, R. H. (1992). GPS meteorology: Remote sensing of atmospheric water vapor using the global positioning system. *Journal of Geophysical Research: Atmospheres*, *97*(D14), 15787–15801. https://doi.org/10.1029/92JD01517

Blewitt, G., Hammond, W. C., & Kreemer, C. (2018). Harnessing the GPS data explosion for interdisciplinary science. *Eos*, *99*. https://doi.org/10.1029/2018EO104623

Boehm, J., Werl, B., & Schuh, H. (2006). Troposphere mapping functions for GPS and very long baseline interferometry from European Centre for Medium-Range Weather Forecasts operational analysis data. *Journal of Geophysical Research*, *111*, B02406. https://doi.org/10.1029/2005JB003629

Choy, S., Wang, C.-S., Yeh, T.-K., Dawson, J., Jia, M., & Kuleshov, Y. (2015). Precipitable water vapor estimates in the Australian region from ground-based GPS observations. *Advances in Meteorology*, *2015*, 956481. https://doi.org/10.1155/2015/956481

Davis, J. L., Herring, T. A., Shapiro, I. I., Rogers, A. E. E., & Elgered, G. (1985). Geodesy by radio interferometry: Effects of atmospheric modeling errors on estimates of baseline length. *Radio Science*, *20*(6), 1593–1607. https://doi.org/10.1029/RS020i006p01593

Gurbuz, G., Jin, S., & Mekik, C. (2015). Sensing Precipitable Water Vapor (PWV) using GPS in Turkey – validation and variations. *Satellite Positioning – Methods, Models and Applications*. https://doi.org/10.5772/60025

Isioye, O. A., Combrinck, L., & Botai, J. O. (2017). Retrieval and analysis of precipitable water vapour based on GNSS, AIRS, and reanalysis models over Nigeria. *International Journal of Remote Sensing*, *38*(20), 5710–5735. https://doi.org/10.1080/01431161.2017.1346401

Isioye, O. A., Combrinck, L., & Botai, J. (2015). Performance evaluation of blind tropospheric delay correction models over Africa. *South African Journal of Geomatics*, *4*(4), 502–525. https://doi.org/10.4314/sajg.v4i4.10

Isioye, O. A., Combrinck, L., & Botai, J. (2016). Modelling weighted mean temperature in the West African region: Implications for GNSS meteorology. *Meteorological Applications*, *23*(4), 614–632. https://doi.org/10.1002/met.1584

Isioye, O. A., Combrinck, L., Botai, J. O., & Moses, M. (2019). Assessing the impact of variations in atmospheric water vapour content over Nigeria from GNSS measurements. *South African Journal of Geomatics*, *8*(1), 27. https://doi.org/10.4314/sajg.v8i1.3

Jade, S., & Vijayan, M. S. M. (2008). GPS-based atmospheric precipitable water vapor estimation using meteorological parameters interpolated from NCEP global reanalysis data. *Journal of Geophysical Research: Atmospheres*, *113*(D3). https://doi.org/10.1029/2007JD008758

Jiang, P., Ye, S., Chen, D., Liu, Y., & Xia, P. (2016). Retrieving precipitable water vapor data using GPS zenith delays and global reanalysis data in China. *Remote Sensing*, *8*(5), 389. https://doi.org/10.3390/rs8050389

Kottek, M., Grieser, J., Beck, C., Rudolf, B., & Rubel, F. (2006). World map of the Köppen-Geiger climate classification updated. *Meteorologische Zeitschrift*, *15*(3), 259–263. https://doi.org/10.1127/0941-2948/2006/0130

Landskron, D., & Böhm, J. (2018). VMF3/GPT3: Refined discrete and empirical troposphere mapping functions. *Journal of Geodesy*, *92*(4), 349–360. https://doi.org/10.1007/s00190-017-1066-2

Leggett, R. W., & Williams, L. R. (1981). A reliability index for models. *Ecological Modelling*, *13*(4), 303–312. https://doi.org/10.1016/0304-3800(81)90034-X

Mengistu Tsidu, G., Blumenstock, T., & Hase, F. (2015). Observations of precipitable water vapour over complex topography of Ethiopia from ground-based GPS, FTIR, radiosonde and ERA-Interim reanalysis. *Atmospheric Measurement Techniques*, *8*(8), 3277–3295. https://doi.org/10.5194/amt-8-3277-2015

Ojigi, L. M., & Opaluwa, Y. D. (2019). Monitoring atmospheric water vapour variability over Nigeria from ERA-Interim and NCEP reanalysis data. *SN Applied Sciences*, *1*(10), 1159. https://doi.org/10.1007/s42452-019-1177-x

Saastamoinen, J. (1972). Atmospheric correction for the troposphere and stratosphere in radio ranging satellites. In *The use of artificial satellites for geodesy* (pp. 247–251). American Geophysical Union (AGU). https://doi.org/10.1029/GM015p0247

Shcherbakov, M. V., Brebels, A., Shcherbakova, N. L., Tyukov, A. P., Alex, T., Janovsky, R., & Kamaev, V. A. (2013). A survey of forecast error measures. *World Applied Sciences Journal (Information Technologies in Modern Industry, Education & Society*, *24*, 171–176.

Ssenyunzi, R. C., Oruru, B., D'ujanga, F. M., Realini, E., Barindelli, S., Tagliaferro, G., von Engeln, A., & van de Giesen, N. (2020). Performance of ERA5 data in retrieving Precipitable Water Vapour over East African tropical region. *Advances in Space Research*, *65*(8), 1877–1893. https://doi.org/10.1016/j.asr.2020.02.003

Wessel, P., Luis, J. F., Uieda, L., Scharroo, R., Wobbe, F., Smith, W. H. F., & Tian, D. (2019). The generic mapping tools version 6. *Geochemistry, Geophysics, Geosystems*, *20*(11), 5556–5564. https://doi.org/10.1029/2019GC008515

Xiaoming, L., Lisheng, X., Yansong, F., Yujie, Z., Jilie, D., Hailei, L., & Xiaobo, D. (2010). Estimation of the precipitable water vapor fom ground-based GPS with GAIT/GLOBK. In *2010 Second LITA International Conference on Geoscience and Remote Sensing*. https://doi.org/10.1109/IITA-GRS.2010.5603260

Yang, H., He, C., Wang, Z., & Shao, W. (2019, June). Reliability analysis of European ERA5 water vapor content based on ground-based GPS in China. In *Proceedings of the 2019 International Conference on wireless communication, network and multimedia engineering (WCNME 2019)* (pp. 44–49). Atlantis Press. https://doi.org/10.2991/wcnme-19.2019.11

Zhang, W., Zhang, H., Liang, H., Lou, Y., Cai, Y., Cao, Y., Zhou, Y., & Liu, W. (2019). On the suitability of ERA5 in hourly GPS precipitable water vapor retrieval over China. *Journal of Geodesy*, *93*(10), 1897–1909. https://doi.org/10.1007/s00190-019-01290-6